Rheol Acta 37:223–233 (1998)

ORIGINAL CONTRIBUTION

Christophe Baravian
Daniel Quemada

Using instrumental inertia in controlled stress rheometry

Received: 4 September1997
Accepted: 13 January 1998

C. Baravian (✉)
LEMTA – Laboratoire d'Energétique
et de Mécanique Théorique et Appliquée
CNRS-UMR 7563
Institut Polytechnique de Loraine
2, avenue de la forét de Haye, BP 160
54504 Vandoeuvre Lès Nancy
France

D. Quemada
LBHP – Laboratoire de Biorhéologie
et d'Hydrodynamique Physico-chimique
CNRS-LA 343
Université Paris 7
2 place Jussien
75251 Paris
France

Abstract We describe a new method for characterizing the non-linear behavior of complex fluids at both small and large deformations. For creep measurements, we use the coupling between the instrumental inertia and the material's elasticity to follow the rheological behavior of a solution of iota carrageenan both above and below the yield stress. It is shown that this coupling selectively excites one particular frequency of the relaxation spectrum. An analytical calculation is used to quantify the non-linear behavior near the yield stress. The "free" oscillations observed during the first few seconds allow us to choose the most appropriate mechanical model. Comparison with experiment shows that even above the yield stress, a linear model can still give independently reliable information about the changes in each element of the mechanical model. A comparison of free and forced oscillations in controlled stress rheometry shows both experimentally and theoretically the conditions under which the use of free oscillations is advantageous.

Key words Inertia effects – free oscillations – controlled stress rheometry – creep test – unsteady measurements

Introduction

In general, it is extremely difficult to study experimentally the non-linear viscoelastic behavior of thixotropic materials. When the times characterizing thixotropy and viscoelasticity are similar, very few methods can separate the effects of these two phenomena. However, when their characteristic times are very different, the structural modifications associated with these two kinds of behavior can be studied independently. Nevertheless, even when thixotropy and viscoelasticity occur on separable times scales, they cannot both be characterized by the same type of experiment.

Studying viscoelasticity using dynamic measurements is limited to the linear behavior, as interpretation of the results is very difficult when non-linear behavior, such as the sol-gel transition, occurs. In flow experiments, partially irreversible destruction of the material often occurs making the comparison between different rheological tests difficult. These problems motivated us to define rheological measurements giving as much information as possible. We show here how a careful analysis of creep measurements made with a controlled stress rheometer can be very useful for the rheological characterization of a complex fluid: a physical gel both above and below its yield stress. Non-linear viscoelasticity was studied using the "free" oscillations generated in the material by applying a stress step. The analysis of such oscillations generated by steps in shear rate has been used for the calculation of the elastic moduli G' and G'' in the linear domain (see Hopkins, 1963, for instance). Many other studies have followed this first analysis for the calculation of the complex modulus (Struik, 1967; Roscoe, 1969). Ferry (1980) has reviewed this work.

A recent study of free oscillations observed in creep experiments suggested application of the same analysis as that used for steps in shear rate (Zölzer and Eicke,

1993), using as usual the frequency and damping of the oscillations for the calculation of the instantaneous and delayed elastic moduli.

Viscoelastic materials generally have broad relaxation spectra. However, in our experiments the coupling of the instrumental inertia with the sample's viscoelasticity results in the selection of one particular frequency. Therefore, a simple mechanical model with a single relaxation time can be used to model the shear strain-time curves.

We propose here an analytical calculation which correctly models the observed behavior in both the linear and non-linear domains. We use a Kelvin-Voigt mechanical model and follow the changes occurring in the different mechanical elements when approaching the yield stress. Once the gel had yielded, it was still possible to study rheological changes in the material with a Maxwell-Jeffreys model and to characterize its viscoelasticity and thixotropy independently.

Instrumental inertia and viscoelasticity: application to the Maxwell-Jeffreys model

We show here how viscoelasticity and instrumental inertia are coupled.

The equation of motion

The equation of motion for the mobile part of the apparatus is:

$$I\frac{\partial \Omega_w}{\partial t} = \Gamma_a - \Gamma_w \tag{1}$$

where Γ_a and Γ_w are respectively the applied and the resistant torque at the moving wall, I is the inertia momentum of the mobile part of the apparatus and Ω_w is the angular velocity.

In linear viscoelasticity, space and time variables naturally separate in the constitutive equation, leading to proportionality between shear rate and angular velocity (proportionality factor $F_{\dot\gamma}$) and shear stress and torque (proportionality factor F_σ). Equation (1) can then be rewritten:

$$a\ddot\gamma_w = \sigma_a - \sigma_w \tag{2}$$

where

$$a = I\frac{F_\sigma}{F_{\dot\gamma}}\ .$$

The constitutive equation

Equation (2), written for the mobile part of the apparatus, is coupled to the constitutive law of the material. We choose a Maxwell-Jeffreys model:

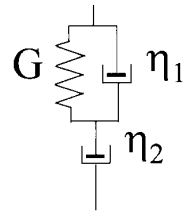

$$(\eta_1+\eta_2)\dot\sigma + G\sigma = \eta_2 G\dot\gamma + \eta_1\eta_2\ddot\gamma \tag{3}$$

Coupling Eqs. (2) and (3) for an applied shear stress step of amplitude σ_0, the following expression can easily be found at the moving wall:

$$(\eta_1+\eta_2)\ddot\sigma + \left(G+\frac{\eta_1\eta_2}{a}\right)\dot\sigma + \frac{G\eta_2}{a}\sigma = \frac{G\eta_2}{a}\sigma_0 h(t) + \frac{\eta_1\eta_2}{a}\sigma_0\,\delta(t) \tag{4}$$

where $h(t)$ is the Heaviside distribution function and $\delta(t)$ is the Dirac delta impulsion.

Remarks on the significance of oscillations

We want to emphasize that any elastic term coupled to Eq. (2) can lead to an oscillating solution, whereas purely viscous materials cannot give rise to oscillations. This distinction cannot be made using controlled shear rate rheometers, as a torsion torque is generally present (see, for instance, Mackay et al., 1992), so that even inelastic materials can give rise to oscillations. For a controlled stress rheometer, it can be asserted that if oscillations occur in creep mode, the material necessarily has elastic behavior. Analysis of these oscillations is relevant whatever the amplitude of the applied shear stress.

Analytical solution of the Maxwell-Jeffreys model

The solution of Eq. (4) splits into two cases: an oscillating solution and a non-oscillating one.

Condition for the existence of oscillations

For the Maxwell-Jeffreys model, the critical case is given by:

$$\frac{\eta_2 G}{a(\eta_1+\eta_2)} - \mathrm{A}^2 \geq 0 \tag{5}$$

with $A=\frac{aG+\eta_1\eta_2}{2a(\eta_1+\eta_2)}$. The associated critical elasticity is then:

$$G \geq G_{\mathrm{critical}} = \frac{2\eta_2^2}{a}\left(1+\frac{\eta_1}{2\eta_2}+\sqrt{1+\frac{\eta_1}{\eta_2}}\right) \tag{6}$$

It is therefore possible to choose the coefficient a (via the geometry used and its inertia) so that a given material will give rise to oscillations.

Solution of Eq. (4) gives:

For $G \geq G_{\text{critical}}$:

$$\sigma_w(t) = \sigma_0\left\{1 - e^{-At}\left[\cos(\omega t) + \frac{aG - \eta_1\eta_2}{2a\omega(\eta_1\eta_2)}\sin(\omega t)\right]\right\} \tag{7}$$

with $\omega = \sqrt{\frac{\eta_2 G}{a(\eta_1+\eta_2)} - A^2}$.

The shear rate is obtained by integration of Eq. (2) with Eq. (7):

$$\dot{\gamma}_w(t) = \frac{\sigma_0}{\eta_2}\left\{1 - e^{-At}\left[\cos(\omega t) + \frac{1}{a\omega}(\alpha A - \eta_2)\sin(\omega t)\right]\right\} \tag{8}$$

The deformation is easily obtained by integration of Eq. (8):

$$\gamma_w(t) = \sigma_0\left\{\frac{t}{\eta_2} - B + e^{-At}\left[B\cos(\omega t) + \frac{A}{\omega}\left(B - \frac{1}{A\eta_2}\right)\sin(\omega t)\right]\right\} \tag{9}$$

with $B = \frac{a(\eta_1+\eta_2)}{\eta_2 G}\left(\frac{2A}{\eta_2} - \frac{1}{a}\right)$ and $\gamma(0) = 0$.

The solution to the non-oscillating case, $G < G_{\text{critical}}$, can be obtained from these equations by replacing the sine and cosine functions by the corresponding hyperbolic functions.

Solutions for the Maxwell and Kelvin-Voigt models

These can be obtained as simplifications of the Maxwell-Jeffreys solution.

The Maxwell model

In this model η_1 tends to zero, so the expression for the critical elasticity, Eq. (6), reduces to:

$$G_{\text{critical}} = \frac{4\eta_2^2}{a} \tag{10}$$

Equations (7)–(9) reduce to, respectively:

$$\sigma_w = \sigma_0\left\{1 - e^{-\frac{G}{2\eta_2}t}\left[\cos(\omega t) + \frac{G}{2\eta_2\omega}\sin(\omega t)\right]\right\} \tag{11}$$

$$\dot{\gamma}_w = \frac{\sigma_0}{\eta}\left\{1 - e^{-\frac{G}{2\eta_2}t}\left[\cos(\omega t) + \frac{1}{\omega}\left(\frac{}{2\eta_2} - \frac{\eta_2}{a}\right)\sin(\omega t)\right]\right\} \tag{12}$$

and

$$\gamma_w = \frac{\sigma_0}{\eta_2}\left\{t - \frac{a}{G}\left(\frac{G}{\eta_2} - \frac{\eta_2}{a}\right)\left[1 - e^{-\frac{G}{2\eta_2}t}\left(\cos(\omega t) + \frac{G}{2\eta_2\omega}\,\frac{G/\eta_2 - 3\eta_2/a}{G/\eta_2 - \eta_2/a}\sin(\omega t)\right)\right]\right\} \tag{13}$$

with $\omega = \sqrt{\frac{G^2}{4\eta_2^2} - \frac{G}{a}}$.

The non-oscillating case is again obtained by replacing the sine and cosine functions by the corresponding hyperbolic functions.

The Kelvin Voigt model

In this model η_2 tends to infinity, so the expression for the critical elasticity, Eq. (5), reduces to:

$$G_{\text{critical}} = \frac{\eta_1^2}{4a} \tag{14}$$

Equations (7)–(9) reducte to, respectively:

$$\sigma_w = \sigma_0\left\{1 - e^{-\frac{\eta_1}{2a}t}\left[\cos(\omega t) - \frac{\eta_1}{2a\omega}\sin(\omega t)\right]\right\} \tag{15}$$

$$\dot{\gamma}_w = \frac{\sigma_0}{a\omega}e^{-\frac{\eta_1}{2a}t}\sin(\omega t) \tag{16}$$

and

$$\gamma_w(t) = \frac{\sigma_0}{G}\left\{1 - e^{-\frac{\eta_1}{2a}t}\left[\cos(\omega t) + \frac{\eta_1}{2a\omega}\sin(\omega t)\right]\right\} \tag{17}$$

with $\omega = \sqrt{\frac{G}{a} - \left(\frac{\eta_1}{2a}\right)^2}$.

The main advantage of this analytical approach is that no hypothesis is necessary concerning limited deformation or dissipation, which is not the case for classical dynamic experiments. Moreover, as long as the proportionality between both shear rate and angular velocity and shear stress and torque remain valid, a similar approach can be adopted for any constitutive equation.

In the next section, this analysis is applied to a physical gel above and below its yield stress.

Results and experiments

Measurements were performed using a Carrimed CS 100 rheometer fitted with a coaxial cylindrical geometry. The creep mode allowed acquisition of 10 points per time decade from 10^{-4} s. The material studied was iota carrageenan, which is a gelling polysaccharide used in the food industry. The sample was provided by Systems Bio-Industries (Carentan, France) and was used at a concentration of 5 g/l in 0.2 M NaCl solution. The manufacturer gave the mass-average molecular weight as 350 000, determined using gel permeation chromatography coupled to refractive index and multiangle light-scattering detectors. As usual, it contained a fraction of kappa carrageenan, estimated as about 7% by the method of Parker et al. (1993). However, under the electrolyte conditions used here, kappa carrageenan does not gel at 20 °C (Parker et al., 1993), so it is not expected to influence the results. The solution was heated at 90 °C for 30 min to achieve complete dissolution, before being placed in the rheometer and cooled to 20 °±0.1 °C. Under these conditions, iota carrageenan undergoes a thermally reversible sol-gel transition close to 60 °C (Parker et al., 1993). Evaporation was prevented by a system specially designed in the laboratory which saturated the air in contact with the sample with moisture.

A series of shear stress steps with increasing amplitudes was applied. The first step had an amplitude of 1 Pa and the increment between steps was also 1 Pa. Creep and recovery curves were each recorded for 20 s. For this length of experiment, a yield stress was observed between 15 and 16 Pa. The Kelvin-Voigt model was therefore used for the experiments with stresses between 1 and 15 Pa. Above this stress, the sample started to flow. Yield was considered to have occurred when recovery was incomplete (to within the resolution of the apparatus, 10^{-3} radians). At this point we considered the sample to be a viscoelastic liquid, and modelled its rheological behavior using the Maxwell-Jeffreys model. Ten successive experiments were then performed at 16 Pa to follow the time-dependent non-linear behavior of the product above this yield stress.

Measurements below the yield stress (Kelvin-Voigt model)

We will not discuss here whether the yield stress really exists or not. We just consider that its value is related to the solicitation time (Cheng, 1986). Our experimental time was chosen in order to obtain observable thixotropic effects over times short enough to limit the irreversible behavior induced by breakdown of the material under shear. This time (typically 10 s) is also comparable with the characteristic thixotropic times obtained for identical solutions of iota carrageenan after extensive shear had removed their elasticity (Baravian et al., 1996).

Figure 1 shows a typical result obtained below the yield stress (i.e., for creep curves from 1 to 15 Pa).

Figures 2 and 3 show the excellent agreement between the Kelvin-Voigt model and experiment data obtained below the yield stress. Only two parameters are open in this fit (G and η_1). Nevertheless, the model correctly describes the frequency shift, the period and the damping of oscillations, the start-up before oscillations and the final deformation.

The recovery curve (Fig. 3) is modelled independently using $\sigma_a = \sigma_0(1-h(t))$ in Eq. (2) and the same method of solution. The initial deformation was taken as the final point on the creep curve.

In the following experiments, the shear stress was incremented until the recovery was different from zero (to within the resolution of the apparatus). The model parameters found are shown as a function of the applied shear stress for both creep and recovery curves in Figs. 4 and 5.

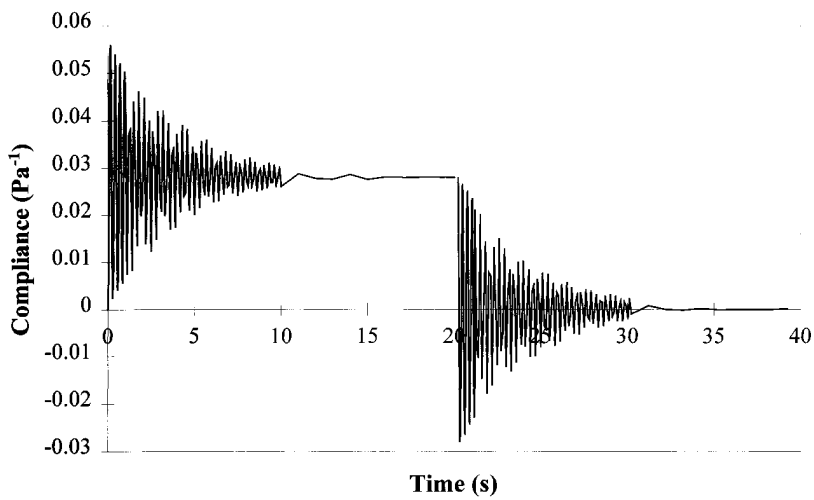

Fig. 1 Typical experimental creep curve. Applied shear stress: 2 Pa

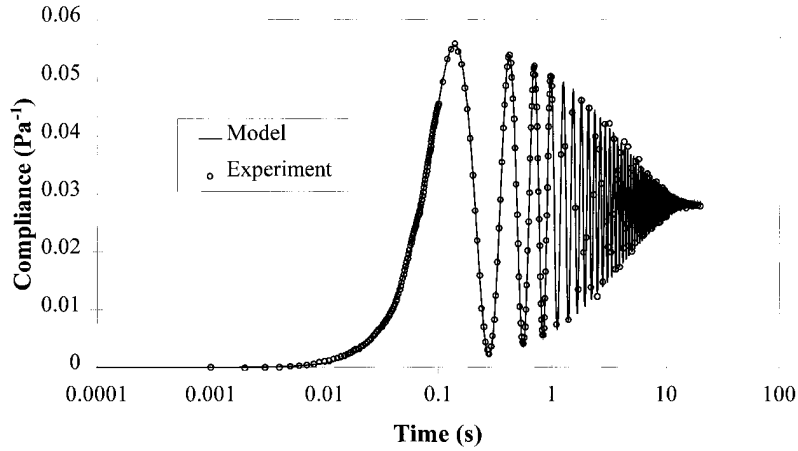

Fig. 2 Creep curve. Applied shear stress: 2 Pa. Comparison between experiment and model (Eq. (17)). $\alpha = 0.06$ Pa·s^{-2}, $G = 35.33$ Pa and $\eta_1 = 0.033$ Pa·s^{-2}

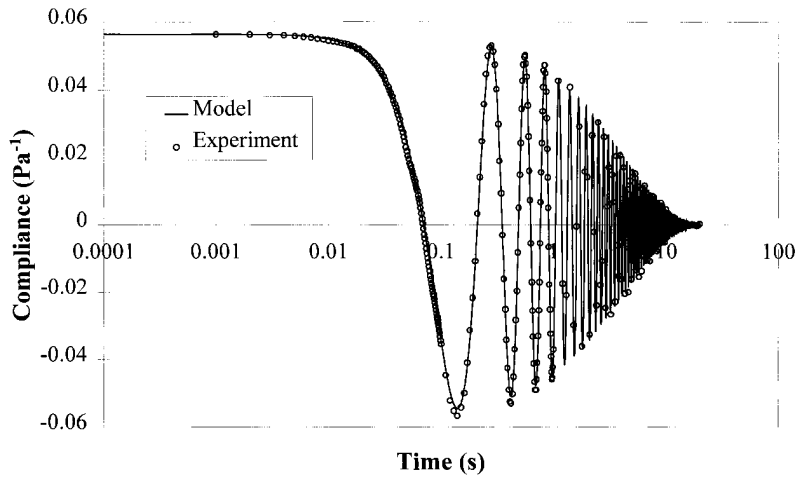

Fig. 3 Recovery curve. Applied shear stress: 2 Pa. Comparison between experimental and model. $\alpha = 0.06$ Pa·s^{-2}, $G = 35.24$ Pa and $\eta_1 = 0.033$ Pa·s^{-2}

In Figs. 4 and 5, the last points (made at 16 Pa) are measured above the yield stress. The data were therefore fitted using the Maxwell-Jeffreys model (Eq. (9)). Both Figs. 4 and 5 show that even below the yield stress, the material was very non-linear. The increase of the elastic modulus under shear was probably due to strain hardening. Similar effects have recently been reported for another physical gel, gelatin (Groot et al., 1996). The viscosity associated to the Kelvin-Voigt element increased slightly with the initial strain both for creep and recovery experiments. They remained nearly equal until a shear stress of 10 Pa was applied. Their separation at higher initial strains may be interpreted in two ways: Either i) yield actually occurred but the resolution of the apparatus prevented its observation (so yield would have been observed if the stress had been applied for longer) or ii) it corresponds to an increase in the non-linearity of the network structure close to the yield stress.

Note that these non-linear effects were reversible below the yield stress. After the 13 Pa experiment, a second measurement at 2 Pa was made. The model parameters fitted were identical, to within 2%, to those of the first 2 Pa experiment.

Measurements made close to the transition (Maxwell-Jeffreys Model)

To follow the modifications in the material once yield had occurred, ten successive measurements were made using an applied shear stress of 16 Pa. The results are shown in Fig. 6.

Only the first second's data from the creep and recovery curves shown in Fig. 6 were fitted to the model. As seen on Figs. 10 and 11, for each particular curve, the frequency of oscillations remains constant in time. This shows that here again, only one particular frequency is selected and a linear mechanical model with a single relaxation time still applies. A Maxwell-Jeffreys model has been found to be appropriate. The remarkable fact that the frequency of oscillations is still constant from one experiment to another is discussed below.

Results of the fit are shown in Figs. 7–9.

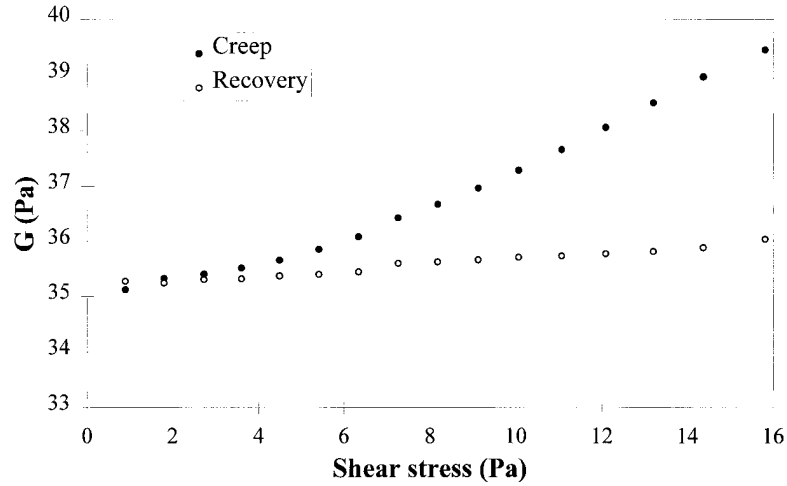

Fig. 4 Elastic modulus from the Kelvin-Voigt model as a function of applied shear stress. Measurements made below the yield stress

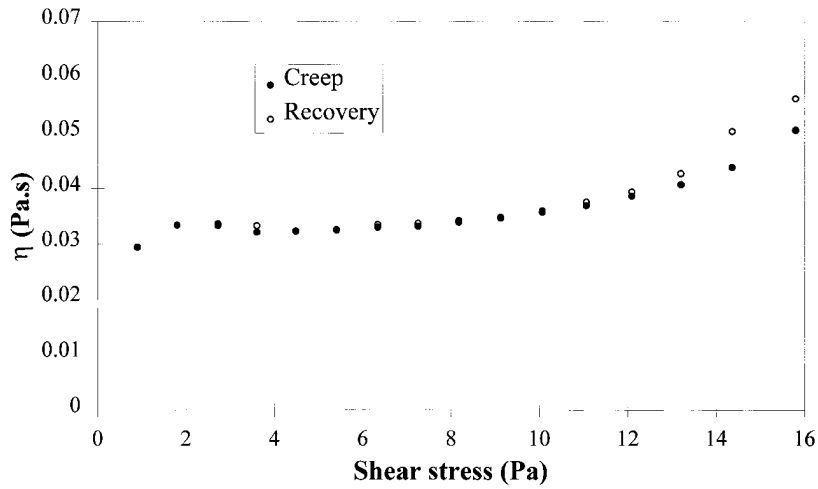

Fig. 5 Viscosity η_1 obtained from the Kelvin-Voigt model as a function of applied shear stress. Measurements made below the yield stress

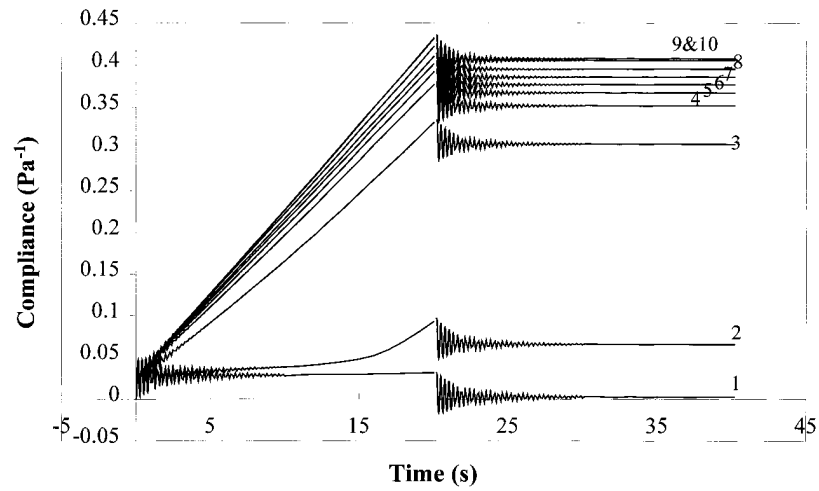

Fig. 6 Successive creep and recovery curves. Applied shear stress: 16 Pa

The main observation is that the material does not lose its elastic properties, even at very high deformations. Figure 7 shows that the elasticity remained constant, even though the deformation increased (see Fig. 6). The time dependency seemed to affect the viscosity η_1 associated to the solid part of the material under stress (Fig. 8). However, the value on recovery seems to remain constant and in good agreement with the values obtained below the yield stress (Fig. 5).

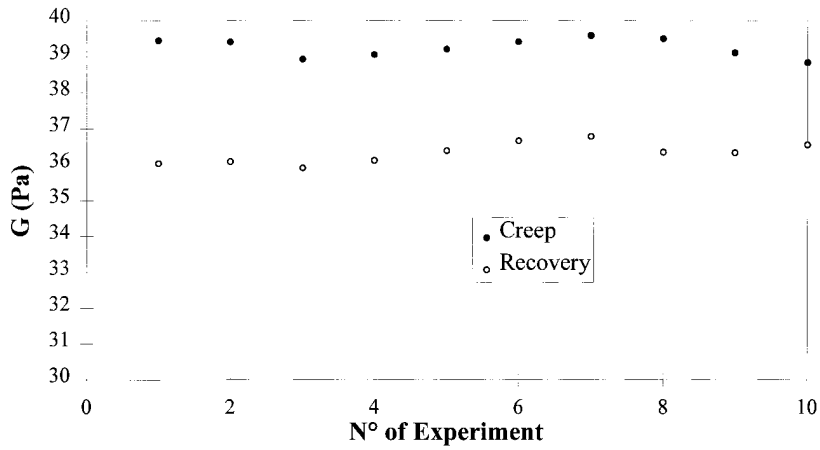

Fig. 7 Elastic modulus vs. the number of applied steps in shear stress of 16 Pa. Measurements made above the yield stress

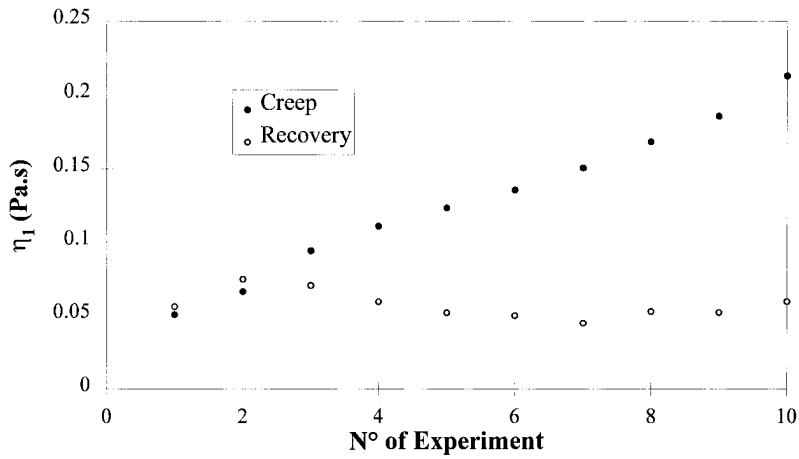

Fig. 8 Viscosity η_1 vs. the number of applied steps in shear stress of 16 Pa. Measurements made above the yield stress

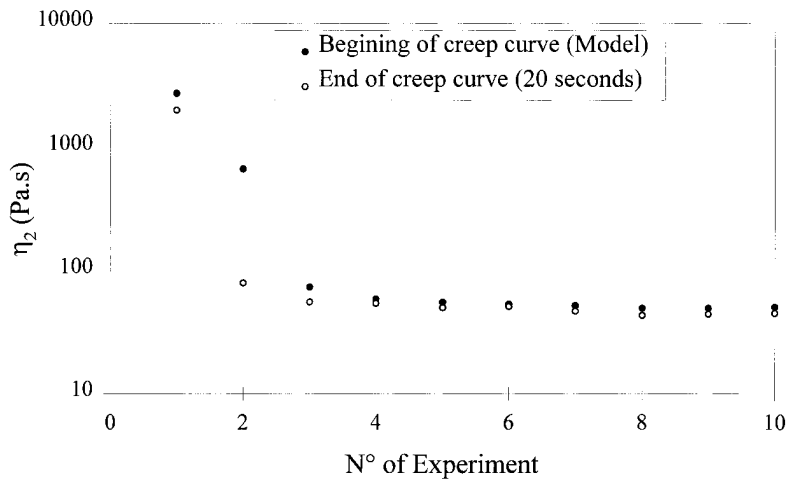

Fig. 9 Viscosity η_2 vs. the number of applied step in shear stress of 16 Pa. Creep curve. Model (initial value) and experiment (viscosity value at 20 s)

Figure 9 shows the variation of the viscosity η_2. As the elasticity remains constant for all successive experiments, the decrease of η_2 can be interpreted as responsible for the change of slope of the creep curves (and especially for the second experiment), that is thixotropy. The latter was also observed via the difference between the initial and final values of the viscosity for the creep curve (Fig. 9). As the number of applied steps increased, the initial and final viscosities reached equilibrium values. The initial viscosity was obtained from the fit of the Maxwell-Jeffreys model to the first second's data. The final viscosity was calculated by numerical differentiation of the deformation-time curve.

An approximate calculation

It seems particularly interesting to try to gain information about the viscoelasticity of a material without having to fit all the data using a particular model. This can be very useful if, for instance, thixotropy occurs at such short times that it affects the period of oscillation. Under these circumstances, the previous analysis is no longer valid. However, an alternative approach, based on direct analysis of the period and damping of the oscillations can be used. The simplifying hypotheses necessary for its use are described below.

Hypothesis: $\eta_2 \gg \eta_1$

When passing the yield stress, it seems reasonable to assume that the flow viscosity is much greater than that associated with the solid element, as was observed here (compare Fig. 8 with Fig. 9). This simplification should also apply to many other types of systems at low shear rates.

Using this simplification, the previously given expressions for A and ω reduce to:

$$A \approx \frac{1}{2}\left(\frac{G}{\eta_2} + \frac{\eta_1}{a}\right) \tag{18}$$

$$\omega \approx \sqrt{\frac{G}{a} - A^2} \tag{19}$$

In this case, the elastic modulus can be determined directly by analysis of the experimental data and determination of the damping and frequency of oscillations through Eq. (19). Struick (1967) gives a "plus" sign in Eq. (19) for generalized viscoelastic models. We consider here that a Maxwell-Jeffreys model is relevant for a large number of materials and therefore use Eq. (19) in the form given above, since it is directly deduced from the exact solution.

Note that the expression for the angular frequency can sometimes be reduced to $\omega \approx \sqrt{\frac{G}{a}}$ if $\frac{G}{a} \gg A^2$. This second hypothesis reduces to $\frac{4\eta_2^2}{a} \gg G \gg \frac{\eta_1^2}{4a}$, so its validity depends on the factor a, which can be varied by the experimenter to some extent. This remark is of interest if a rheometer whose inertia can be modified is available. Note that these conditions apply to the carrageenan solution studied here. This can be seen in Figs. 10 and 11, which show the first second of the creep curves and dimensionless recovery curves shown in Fig. 6.

These figures show that the frequency remained nearly constant. This observation demonstrates that the elasticity was not modified when yield occurred. It also shows once more that only one particular frequency is solicited, the corresponding resonance frequency, which depends mainly on the material elasticity and the inertia and geometry of the apparatus. The next section shows

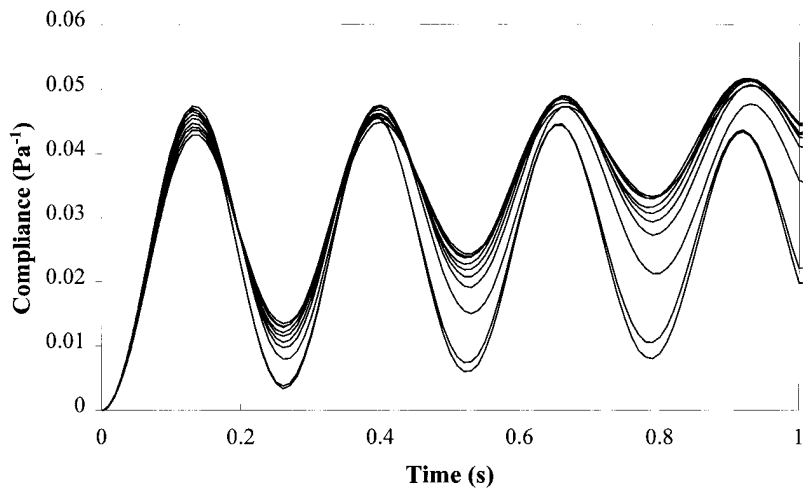

Fig. 10 Representation of the first second of creep curves from Fig. 6. Curves from bottom to top correspond to successive experiments from 1 to 10

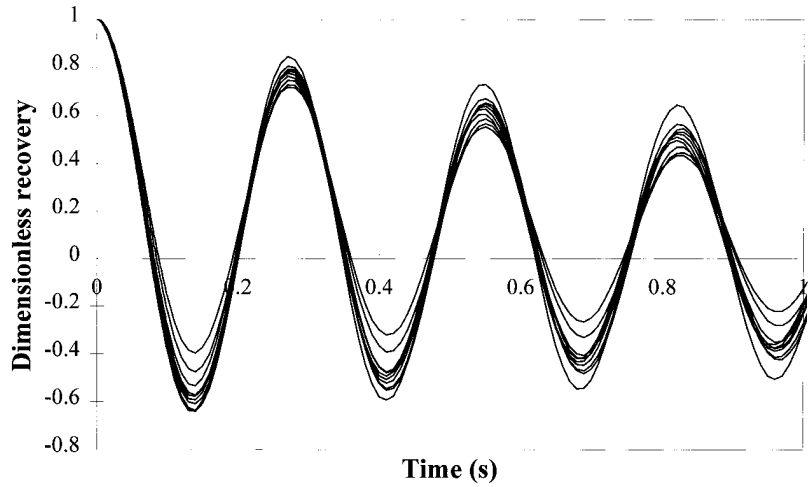

Fig. 11 Dimensionless representation (1 for the first data point to zero for the last one) of the first second of recovery curves from Fig. 6. Curves from higher to lower amplitude correspond to successive experiments from 1 to 10

how different frequencies can be excited by changing the instrumental inertia.

Interpretation of the damping is more difficult since the contributions of viscosities η_1 and η_2 cannot be obviously separated in Eq. (18). However, these dependencies can be separated by i) complete modelling of creep and recovery curves, or ii) by repeating the experiment using different values of the inertia factor a (see Eq. (18)).

The previously cited work of Zölzer and Eicke (1993) makes the assumption that the deformation response follows a logarithmic decrease and a simple oscillating sine variation. They note that to obtain a good fit to their experimental data, two additional arbitrary variables were required: a frequency shift and a superposed linear variation. We think that the method described here of coupling the Maxwell-Jeffreys model with instrumental inertia would have given a more satisfactory alternative approach, since only one extra parameter (η_2) is required to give a complete description of the data, without using any arbitrary variables. Moreover, the parameters used here have a precise physical significance, unlike the arbitrary parameters introduced in their model.

It is important to note that the presence of inertia effects can lead to erroneous extrapolations at short times. In fact, the use of an "average curve" through the oscillations can produce a non-existent instantaneous elasticity at $t=0$ (see Eq. (9) and Fig. 1). However, if both previous simplifying hypothesis apply, this extrapolation can give quite a good estimate of the material elasticity. Nevertheless, this method should be used with care.

Comparison with forced oscillations

This section compares "free" and forced oscillations and demonstrates the possible use of the analysis described here to extend the frequency range covered by forced oscillations. The latter is always very limited in controlled stress rheometers.

In general, the ability to modify the oscillation frequency (and therefore select a different mode) depends on the material under test and in particular depends strongly on its elasticity. The parameter a can be modified by changing the instrumental inertia. This method is preferable to changing the geometry, as each sample can be tested at many values of a. We have designed a simple system for adding a mass to the mobile part of the rheometer. An increase in inertia leads to a decrease in the oscillation frequency, and its maximum value depends on the sample and the rheometer inertia without any additional mass.

The frequency range of dynamic oscillations is limited in controlled stress rheometers by inertia effects. Methods to correct data for these effects are available, but their use is limited, as can be seen in Fig. 12, which shows a comparison of dynamic and "free" oscillations for an applied shear stress of 1 Pa. The data points were calculated using both creep and recovery data. Above a frequency of about 3 Hertz, the dynamic mode shows a shift in the loss angle, which rapidly increases to 180°. This shift is a tyical effect of instrumental inertia, giving erroneous results, especially for G'. A rough estimate of the frequency at which inertia will give incorrect results in the dynamic mode can be obtained by calculating the resonant frequency using $\mathrm{f}_{\mathrm{res}} = \frac{\omega_{\mathrm{res}}}{2\pi} \approx \frac{\sqrt{G/a}}{2\pi}$. This calculation gives $f_{res} \approx 3$ Hertz, in good agreement with the frequency at which the shift of the loss angle occurs in Fig. 12. The free oscillation mode gives values in good agreement with the forced oscillations below this frequency. This shows the validity of the proposed approach, using a simple mechanical model for the description of "free" oscillations in creep and recovery curves.

For materials with significant elasticity, higher frequencies can be attained when oscillations are free than

when they are forced, as can be seen in Fig. 13 which shows results for a silicon gel made in situ. In this case, the dynamic mode remains valid over the whole frequency range available (up to 40 Hz), since the resonant frequency is about $f_{res} \approx \frac{\sqrt{G/a}}{2\pi} \approx 75$ Hz. Since the sample remains solid, a Kelvin-Voigt model was used for the modeling of oscillations in creep mode.

Conclusions

The method described here, based on a careful analysis of the coupling between instrumental inertia and material elasticity, is used to characterize shear-induced modifications of a thixotropic non-linear material both above and below its yield stress. For creep experiments, this coupling automatically selects on particular frequency and simple mechanical models can therefore be used for the description of experimental curves. This approach is shown to provide a powerful tool for the characterization of non-linear viscoelasticity.

Furthermore, it has been shown that the frequency of the "free" oscillations observed in creep experiments can be modified at will by altering the rheometer's inertia. Under suitable conditions, this method extends the frequency range accessible using controlled stress rheometers. In dynamic mode, this range is very limited for these instruments. In addition, measurements are also extended into non-linear regimes and large deformations. This method could easily be implemented as a complement to dynamic oscillations in existing stress-controlled rheometers.

This approach should open new perspectives for the rheological characterization of complex fluids under unsteady conditions.

Acknowledgements We would like to thank Alan Parker for his linguistic assistance and suggestions.

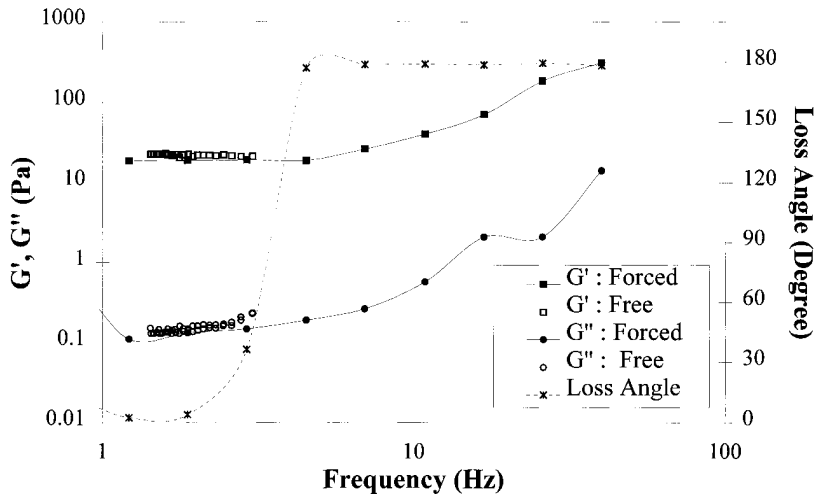

Fig. 12 Comparison between forced and free oscillations. Iota-carrageenan gel. Applies shear stress: 1 Pa

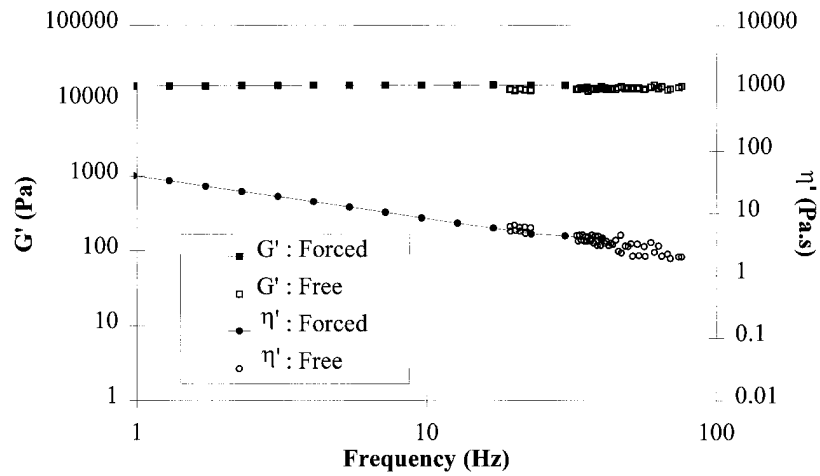

Fig. 13 Comparison between forced and free oscillations for a silicon gel. Maximum frequency obtained using the creep mode $\approx$75 Hz. Applied shear stress: 100 Pa

References

Baravian C, Quemada D, Parker A (1996) Modelling thixotropy using a novel structural kinetics approach: Basis and application to iota carrageenan. J Texture Studies 27:371

Cheng DCH (1986) Yield stress: a time dependent property and how to measure it. Rheol Acta 25:542

Ferry JD (1980) The Viscoelastic Properties of Polymers. Wiley, New York Chichester Brisbane

Groot RD, Bot A, Agterof WGM (1996) Molecular theory of strain hardening of a polymer gel: application to gelatin. J Chem Phys 104:9202

Hopkins IL (1963) Iterative calculation of relaxation spectrum from free vibration data. J Applied Polym Sci 7:971

Mackay ME, Liang C-H, Valley PS (1992) Instruments effects on stress jump measurements. Rheol Acta 31:481

Parker A, Brigand G, Miniou C, Trespoey A, Vallée P (1993) Rheology and fracture of mixed ι and κ-carrageenan gels: Two step gelation. Carbohydr Polym 20:253

Roscoe E (1969) Free damped oscillations in viscoelastic materials. J Phys D 2:1261

Struick LCE (1967) Free damped vibrations of linear viscoelastic materials. Rheol Acta 6:119

Zölzer U, Eicke HF (1993) Free oscillatory shear measurements – an interesting application of constant stress rheometers in the creep mode. Rheol Acta 32:104